HIGH SCHOOL EDITION
Journal of Student Research
Volume 13 Issue 2 (2024)

Real-Time Black Ice Detection in Drone View Using YOLOX

Jinhoo Oh[1], Justin Moon[1], Seokhee Han[1] and Donghwan Shin[#]

[1]Cheongshim International Academy, Republic of Korea
[#]Advisor

ABSTRACT

Black ice is a perilous phenomenon resulting from frozen precipitation on road surfaces. It stands as one of the most prominent contributors to winter traffic accidents since it is nearly invisible. Given these characteristics, there is a pressing need to develop automotive systems capable of detecting black ice to improve driving safety and conditions. This study proposes the deployment of two YOLOX-based models to implement real-time black ice detection from drone-view images. The proposed approach leverages YOLOX-Tiny, known for its proficiency in real-time object detection, in conjunction with YOLOX-B which is a refined version designed specifically for detecting black ice on roadways. For training and evaluating the proposed system, we collected a dataset of black ice consisting of 2,851 sample images sized at 416x416 pixels. Significantly, YOLOX-Tiny achieved an AP@[0.5:0.95] of 0.4923, whereas YOLOX-B achieved 0.4779. Additionally, we demonstrate a practical implementation of the proposed method by deploying the system on the Nvidia Jetson Orin Nano device for real-time inference. The black ice dataset we compiled is publicly available on GitHub. We expect that the proposed black ice detection system will contribute to effectively maintaining safer driving conditions.

Introduction

Black ice is a transparent and nearly invisible thin layer of ice that forms on road surfaces, particularly during cold weather conditions. It's called "black" because it often blends in with the pavement which makes it difficult for drivers to see. Black ice typically forms when the air temperature is at or below freezing, causing any moisture on the road, such as melted snow or rainwater, to freeze rapidly.

Black ice stands as a main factor contributing to winter traffic accidents, often forming during the morning when the road surface is sufficiently damp and chilled. In the United States alone, black ice is responsible for over 1,300 fatalities and 116,800 injuries annually (FHWA 2023). Research indicates that the fatality rate for accidents involving black ice is 1.6 times higher than under normal road conditions, underscoring the grave dangers associated with this phenomenon. Accurate detection of black ice is necessary in reducing the number of accidents it causes.

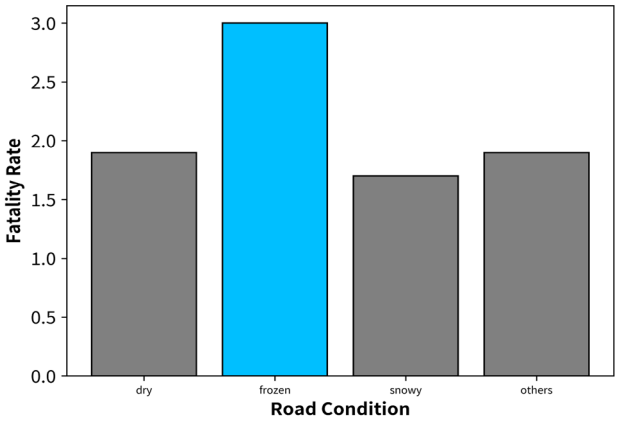

Figure 1. Comparison of Fatality Rates Depending on Road Conditions

The traditional approach for detecting black ice has several disadvantages, due to its time-consuming and labor-intensive nature. Typically, this method involves manual inspections of road surfaces by personnel, which requires significant time and effort. Each inspection involves physically examining the roadways, often during adverse weather conditions, increasing the risk to personnel safety. Moreover, the process is highly reliant on human observation, which can be prone to errors and inconsistencies. Additionally, the need for constant monitoring and manual intervention makes it challenging to cover large areas efficiently, leading to potential delays in identifying and addressing black ice hazards. Overall, the traditional approach's reliance on manual labor makes it inefficient and resource-intensive which highlights the need for more automated and streamlined methods for detecting black ice.

Recently, several machine learning-based studies have introduced methods for automated black ice detection. Lee et al. introduced a black ice detection system based on convolutional neural networks (Lee et al. 2020). Kim et al. developed an object detection system for identifying black ice using infrared cameras (Kim et al. 2021). Li et al. showcased a lightweight convolutional neural network architecture tailored for detecting black ice, specifically designed for Infrared Road environments (Li et al 2021). Zhang et al. proposed a hybrid approach that leverages thermal and RGB images to achieve precise black ice detection (Zhang et al. 2022).

However, previous research utilized antiquated models, making real-time detection on edge devices difficult. Even models reported to have been developed and tested are not reproducible due to the lack of description of the models. In some cases, overfitting is suspected due to the small size of the dataset used in the studies. Some used Google Image Search to collect image data, which is less reliable. Some paid attention to the noise caused when a car passes on black ice for the task. Others analyze the decrease in the spinning of the wheels when passing through black ice. However, a severe limitation exists in these methods: a vehicle must go over black ice to detect it. Thermal cameras have a significant limitation in that they are costly. In some cases, outdated models with longer inference times have been chosen. For studies using YOLO, the cutting-edge object detection model, overfitting may have occurred due to small dataset sizes.

Table 1. Comparison of Previous Research

Researcher	Image Type	Data Collection Method	Dataset Size	Model	Accuracy (Evaluation Metrics)
Lee *et al.*	Digital	Google Image Search	11000	CNN	0.95 (Accuracy)

Kim *et al.*	Infrared	Spray water on asphalt pieces	900	YOLOv4	0.735 (Recall)
Li *et al.*	Digital	Spray water on asphalt pieces	536	1) MobileNetV2 2) Custom machine learning model	1) 0.97 (Accuracy) 2) 0.99 (Accuracy)
Zhang *et al.*	Thermal	Attached a camera to the roof of the vehicle and captured the road surface	4244	CNN	0.94 (Precision)

However, these methods are inefficient because they fail to account for the irregular nature of black ice formation on road surfaces which makes them unsuitable for real-world scenarios. To address this issue, we propose a large scale black ice dataset and the practical implementation of a system for real-time inference. We have collected a large-scale collection of black ice image samples to encompass various geometric patterns and distributions of black ice. Additionally, we have investigated data augmentation techniques to enhance the utility of the dataset. Furthermore, we have introduced a practical implementation of the proposed system on an embedded device for real-time inference. The proposed method achieved an AP@[0.5:0.95] of 0.4923 which demonstrates state-of-the-art performance.

Proposed System

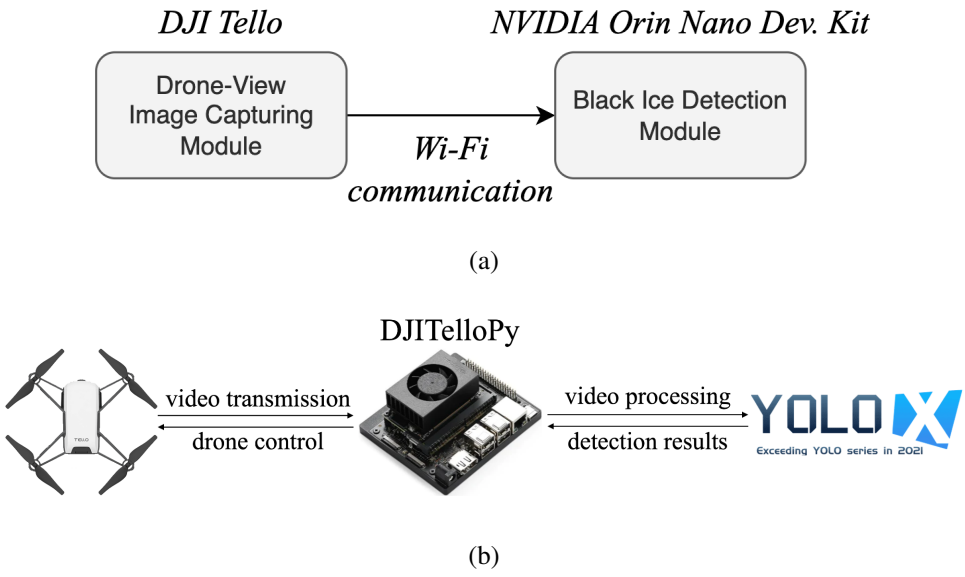

Figure 2. Flowchart of the proposed system. (a): System overview and (b): Implementation details

The proposed system consists of two modules: the drone-view image capturing module and the machine learning-based black ice detection module (Figure 2). The drone-view image capturing module acquires input images

using the camera equipped on the drone, which are then transmitted to the embedded device for black ice detection inference.

In this chapter, we provide detailed explanations of these two modules. The chapter is structured as follows: Chapter 2.1 elaborates on the drone-view image capturing module, while Chapter 2.2 delves into the machine learning-based black ice detection module. Finally, Chapter 2.3 will discuss dataset collection and its statistical analysis.

Drone-View Image Capturing Module

Figure 3. DJI Tello (Bhujbal and Barahate 2022)

This study used DJI's Tello, a drone that is easy to program and convenient for shooting and transmitting images and videos. Its built-in camera can record HD (720p) video in 30 FPS and take 5MP (2592x1936) photos with a field of view (FOV) of 82.6°. The drone measures 98x92.5x41 mm and weighs about 80 grams. The captured image is transferred to the black ice detection module via bluetooth communication. The detailed process of black ice detection will be explained in Chapter 2.

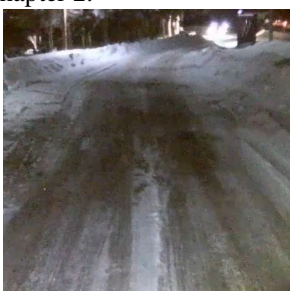

Figure 4. An example black ice image captured using DJI Tello

Black Ice Detection Module

Machine Learning-Based Detection

YOLO (Ge et al. 2021) is the most representative one-stage detector that performs feature extraction and object classification simultaneously. It is known for its fast processing speed and aptness for real-time use.

YOLOX is based on the spatial pyramid pooling layer of YOLOv3 and connects feature pyramid network for prediction. Its feature channel is reduced to 256 using a 1x1 convolutional layer. Both classification and regression are performed using two branches of two 3x3 convolutional layers.

YOLOX provides anchor-free object detection. It is suitable for detecting black ice since it varies in size and shape. CSPDarknet53 is the backbone for YOLOX. This enables more stable learning based on gradient flow than the previous backbone, Darknet53. Newly introduced YOLO-based models have limitations in terms

of black ice detection. YOLOv7 is anchor-based, and YOLOv8 is not sufficiently validated due to a lack of published papers. We concluded YOLOX to be the most suitable for the task since it is easy to modify due to the abundance of past works, such as object detection in low light conditions and aerial images (Wang et al. 2023).

Among YOLOX variants, this research used YOLOX-Tiny for its small model size, which allows the model to be run on Orin in a stable manner. The backbone structure of YOLOX is downsized for YOLOX-Tiny. Based on 416x416 input resolution, the total number of parameters is 5.06M, and GFlops marks 6.45. The number of layers in Darknet is changed, and the number of head channels is reduced to 96.

This research proposes YOLOX-B, a novel model based on YOLOX-Tiny, with improved speed and minimal accuracy loss. The CSP layers in the backbone network are decreased to one, and the number of YOLOX head channels is also reduced to 64.

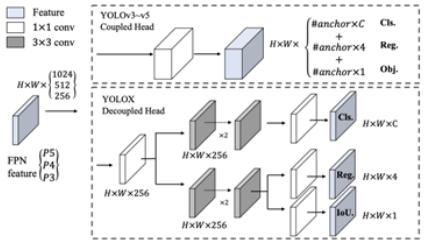

Figure 5. YOLOX Model Architecture (Ge et al. 2021)

Table 2. Overview of Model Training

	YOLOX-Tiny	**YOLOX-B**
Train Dataset	D1: 413 D2: 814 D3: 1,137	
Epoch	300	
Batch Size	32	16
Learning Rate	0.001	
Learning Rate Scheduler	yoloxwarmcos	
Decay Rate	0.0005	
Early Stopping (Y/N)	Y	
Resolution of Input Images	416x416	

Nvidia Jetson Orin Nano Developer Kit

This study adopted NVIDIA's Orin Nano Developer Kit (Orin) to analyze the camera footage from Tello. The kit is built around the NVIDIA Orin system-on-chip (SoC), which is a high-performance computing platform specifically designed for autonomous machines, such as robots, drones, and autonomous vehicles. The installed packages and versions of Orin used to run YOLOX are shown in Table 3.

Figure 6. NVIDIA Orin Nano Dev. Kit (Orin) (Archet et al. 2023)

Table 3. Orin Environment

Type	Name
CPU	ARMv8 Processor rev 1 (v8l)
GPU	NVIDIA GA10B
Memory	8Gb
OS	Ubuntu 20.04.6 LTS
Pytorch Version	2.0.0+nv23.05
TensorRT Version	5.1.2
OpenCV Version	4.8.0 with CUDA

Large Scale Black Ice Dataset

Due to the lack of publicly available black ice image datasets collected on drones, we built our own dataset for this research. The equipment used to construct the dataset is shown in Table 4. Outdoor images were taken with Tello.

Table 4. Camera Equipment

Name	Manufacturer	Location
iPhone SE2	Apple	California, US
iPhone SE3	Apple	California, US
iPhone 12	Apple	California, US
iPhone 14 Pro	Apple	California, US
Q9	LG Electronics	Seoul, South Korea
V30	LG Electronics	Seoul, South Korea
Tello	DJI	Shenzhen, China

The custom datasets were built in three ways, as shown in Table 5. The pictures in the D1 and the D2 datasets were taken indoors. The existence of quality indoor datasets demonstrates the possibility of creating reliable datasets for black ice detection even in seasons other than winter. It also contributes to future works on

black ice detection by building datasets in a controlled laboratory environment, an economical alternative to taking images outside in winter.

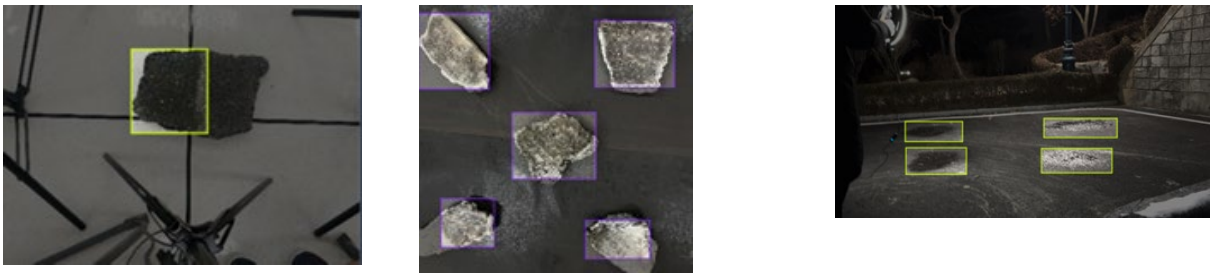

(a) (b) (c)

Figure 7. Sample image for each dataset. (a): D1 dataset, (b): D2 dataset, and (c): D3 dataset

D1 Dataset

Each asphalt piece was frozen to temperatures between -4°C and -20 °C. Black ice was then created by spraying the surface with 4°C tap water and waiting 30 seconds. The water was sprayed on one side of a line that bisects the asphalt piece, leaving a 1 mm thick layer of water on one side. The experimental setup is shown in Figure 8. One camera was placed 1 meter above the asphalt piece, and the other two were placed 1 meter above and 0.50 meters to the left and right. Photos of black ice were taken at 1-minute intervals for 5 minutes, resulting in 18 images for each asphalt piece. The D1 dataset is likely to enhance our model accuracy, for it best reflects the optical properties of black ice, such as light reflection.

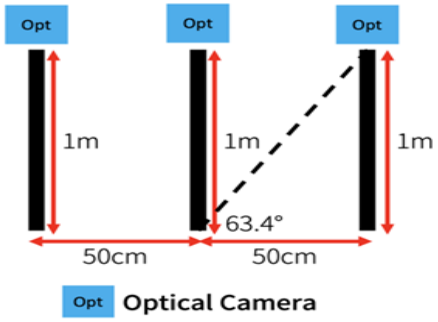

Figure 8. Experimental Setup Design for Obtaining D1 Dataset

D2 Dataset

Each asphalt piece was frozen to temperatures between 4°C and -20°C. Then, 4°C tap water was sprayed at various parts of the piece to form a 1 mm thick sheet of black ice. As shown in Figure 9, the asphalt felt paper attached to a 1.2 m x 1.2 m MDF wood board was used as a background for our dataset to resemble the road surface. Two to five among twenty of the asphalt pieces were randomly selected and placed on the board to depict the arbitrariness of black ice. Videos were taken from a distance of 0.2 to 1.5 meters at an angle of 10° to 90°, similar to drone settings.

The D2 dataset provides a good representation of the environment of black ice on road surfaces since it considers the irregularity of real-world black ice in terms of number, size, and placement.

Figure 9. Asphalt Felt Board

D3 Dataset

1mm thick black ice was created by spraying 4°C tap water on the road in CheongShim International Academy with a surface temperature between 0°C to -6°C. Videos were taken with Tello from 0 AM to 6 AM. The drone was kept parallel and 1 meter above the ground, and videos were recorded from different directions. The D3 dataset is expected to benefit our model accuracy as it provides drone imagery that is highly similar to real-world conditions.

As this study aims for highly accurate black ice detection in drones, we included only the D3 dataset in the Test and Validation sets. The D3 dataset was divided into Train, Validation, and Test sets in the ratio of 7:2:1. The number of images per dataset is shown in Table 5.

Table 5. Number of Train, Validation, and Test Data per Dataset

Dataset	Train	Validation	Test
D1	413	0	0
D2	814	0	0
D3	1,137	325	162

Data augmentation was used during training to prevent overfitting and improve model accuracy. Sample images with mixup, mosaic, HSV (Hue, Saturation, and Value), or all three augmentations are shown in Figure 10.

Mosaic and mixup augmentation were used to befit the model for a wider array of background conditions. HSV augmentation was used to train the model for a broader range of lighting conditions. During training, data augmentation was randomly applied to the images at each iteration, and only for the last 15 epochs was the model trained without data augmentation to stabilize its training.

(a) (b) (c) (d)

Figure 10. Images After Data Augmentation. (a): Mixup, (b): Mosaic, (c): HSV, and (d): All

The distribution of annotation locations can be represented as three heatmaps as shown in figure 11. The D1 dataset, collected with a strict experimental setting, has the annotations focused at the center. The D2 dataset shows the broadest distribution of objects, indicating that it fully illustrates the random nature of black ice formation. The D3 dataset shows a concentration of its annotations in the bottom half of the images as it was collected from droneview.

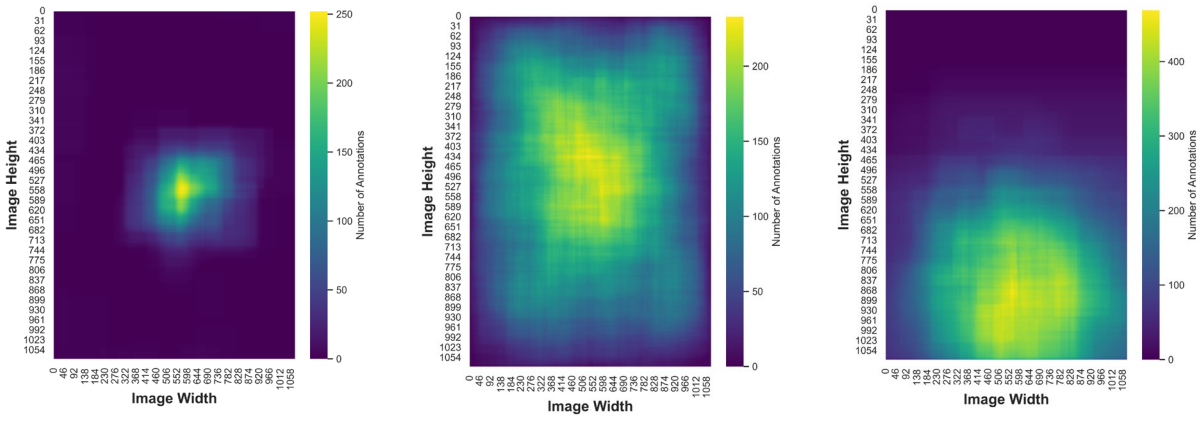

(a) (b) (c)

Figure 11. Dataset Annotation Heatmap. (a): D1 dataset, (b): D2 dataset, and (c): D3 dataset

Experimental Results

Accuracy

Since black ice detection is highly similar to object-detection tasks for medical purposes in terms of research method and purpose, we assessed both models with sensitivity. YOLOX-Tiny has a higher AP@[0.5:0.95]. Although the accuracy of YOLOX-B is relatively low, it demonstrates superiority in its higher 27 FPS, compared to the 24 FPS of YOLOX-Tiny.

Table 6. Model Training Results

Model	AP@[0.5:0.95]	Sensitivity	FPS
YOLOX-Tiny	0.4923	97.2	24
YOLOX-B	0.4779	96.3	27

The precision-recall graphs for each model on our test dataset are as shown in Figuure 12. The graphs show a clear trade-off between precision and recall. The models have achieved high AP numbers, over 0.47, compared to previously trained computer vision models, yet show little signs of overfitting from their precision-recall curves. This ensures their stable performance in further applications as well.

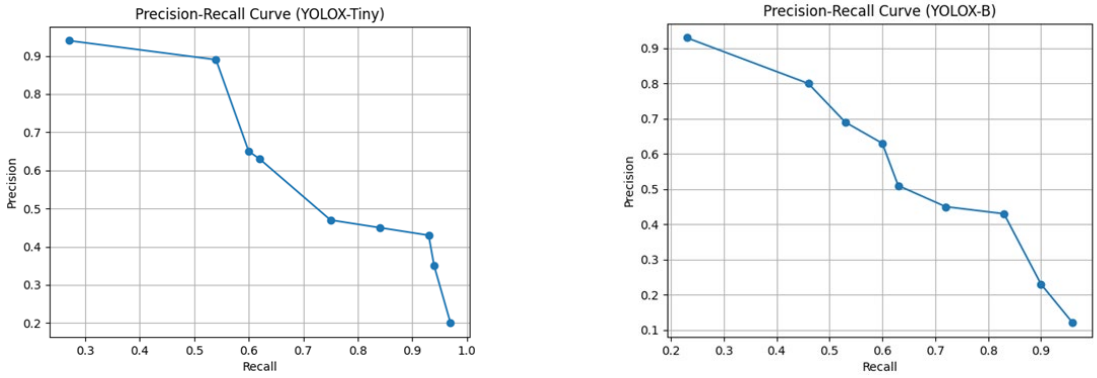

(a) (b)

Figure 12. Precision-Recall Graph. (a): YOLOX-Tiny and (b): YOLOX-B

Hyperparameter Control

Learning Rate

As shown in Table 7, both YOLOX-Tiny and YOLOX-B demonstrated the highest accuracy at a learning rate 0.001. Thus, our team trained the model at a 0.001 learning rate.

Table 7. Variation in Model Performance According to Learning Rate

Model	Base Learning Rate	AP@[0.5:0.95]	Epoch
YOLOX-Tiny	0.01	0.5789	200
	0.001	0.5883	
	0.0001	0.5779	
	0.00001	0.4923	
YOLOX-B	0.01	0.5560	
	0.001	0.5761	
	0.0001	0.5743	
	0.00001	0.0833	

Batch Size

As shown in Table 8, YOLOX-Tiny showed higher accuracy at batch size 32. YOLOX-B performed best at batch size 16. Thus, our team trained the model at 32 batch size for YOLOX-Tiny and 16 batch size for YOLOX-B.

Table 8. Variation in Model Performance According to Batch Size

Model	Batch	AP@[0.5:0.95]	Epoch
YOLOX-Tiny	16	0.603	200
	32	0.6428	
YOLOX-B	16	0.5762	
	32	0.5548	

Epoch

As shown in [Fig 7] and [Fig 8], the losses of models converged at 250~260 epochs. Thus, our team trained the model for 300 epochs.

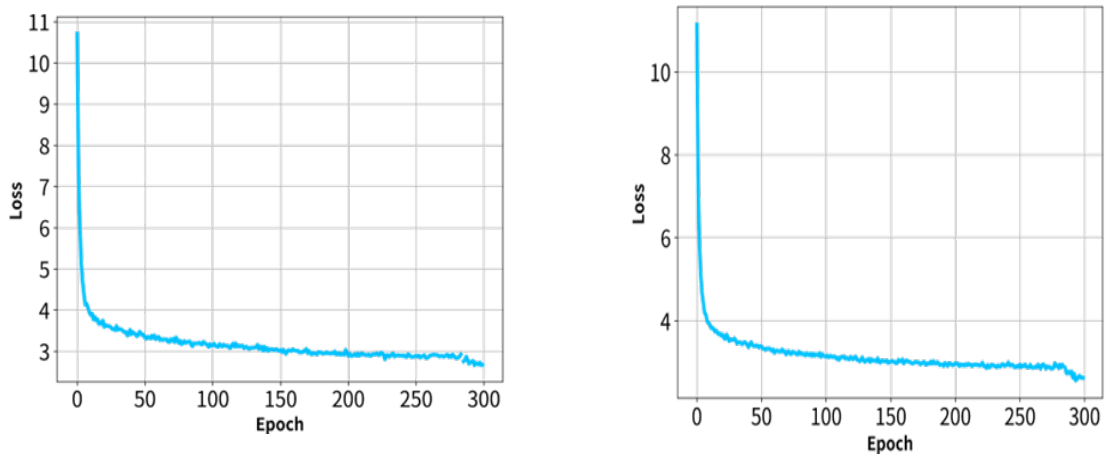

(a) (b)

Figure 13. Convergence of Training Loss. (a): YOLOX-Tiny and (b): YOLOX-Tiny

Resolution

When the model was trained with resolutions of 416x416 and 640x640, respectively, the number of computations for training increased significantly at the higher resolutions. However, there were minor improvements in model accuracy as the resolution increased. We observed that higher resolutions resulted in only a slight improvement in model accuracy, despite a significant increase in computational load. Therefore, we determined the resolution of the input images to be set at 416x416.

Table 9. Gflops for Each Input Image Resolution

Model	Resolution	Gflops	AP@[0.5:0.95]
YOLOX-Tiny	416	6.45	0.6813
	640	15.23	0.6624
YOLOX-B	416	2.7	0.6378
	640	6.4	0.6195

Figure 14. Black Ice Detection Sample Image

Conclusion

This study used YOLOX-Tiny and improved the model to create YOLOX-B to perform real-time black ice detection with drones. Custom black ice datasets were built and analyzed. YOLOX-Tiny marked an AP@[0.5:0.95] of 0.4923 and an FPS of 24 with Orin. On the other hand, YOLOX-B marked an AP@[0.5:0.95] of 0.4779 and an FPS of 27 with the same conditions. Both successfully detected black ice in real time. The study enables real-time black ice detection with drones, which has not been actively studied. It can play a crucial part in reducing traffic accidents caused by black ice. In addition, we collected and released a black ice dataset previously unavailable to the public to support further research. Future works will be conducted to optimize the black ice detection model using model architectures and backbones other than YOLOX-Tiny.

Acknowledgments

I would like to thank my advisor for the valuable insight provided to me on this topic.

References

Ahmad, T., Cavazza, M., Matsuo, Y., & Prendinger, H. (2022). Detecting human actions in drone images using YoloV5 and stochastic gradient boosting. *Sensors*, *22*(18), 7020.

Archet, A., Gac, N., Orieux, F., & Ventroux, N. (2023, June). Embedded AI performances of Nvidia's Jetson Orin SoC series. In *17ème Colloque National du GDR SOC2*.

Bae, T.-w. (2019, Dec 21). “"Black ice" that you can't avoid even when you open your eyes... Even if there is a precautionary measure, it is a huge budget obstacle”: The Korea Economic Daily
https://www.hankyung.com/society/article/201912201477i

Bhujbal, K., & Barahate, S. (2022, May). Custom Object detection Based on Regional Convolutional Neural Network & YOLOv3 With DJI Tello Programmable Drone. In *7th International Conference on Innovation & Research in Technology & Engineering (ICIRTE)*.

FHWA. (2023, Feb 1). “Snow and Ice FHWA Road Weather Management”: The Federal Highway Administration (FHWA)
https://ops.fhwa.dot.gov/weather/weather_events/snow_ice.htm

Gay, D. A., & Davis, R. E. (1993). Freezing rain and sleet climatology of the southeastern USA. *Climate Research*, *3*(3), 209-220.

Ge, Z., Liu, S., Wang, F., Li, Z., & Sun, J. (2021). Yolox: Exceeding yolo series in 2021. *arXiv preprint arXiv:2107.08430.*

Kim, H.G., Jang, .M. S, & Lee, Y. S. (2021). A black ice detection method using infrared camera and YOLO. *Journal of the Korea Institute of Information and Communication Engineering*, 25(12).

Kim, S. (2020). *Methods to cope with thin ice (black ice) on roads in winter in the Netherlands* (pp. 1-24). Korea Transport Institute.

Lee, H., Hwang, K., Kang, M., & Song, J. (2020, December). Black ice detection using CNN for the Prevention of Accidents in Automated Vehicle. In *2020 International Conference on Computational Science and Computational Intelligence (CSCI)* (pp. 1189-1192). IEEE.

Lee, H., Kang, M., Song, J., & Hwang, K. (2020). *The detection of black ice accidents for preventative automated vehicles using convolutional neural networks. Electronics*, *9*(12), 2178.

Li, Y. J., & Kang, S. K. (2021). A Black Ice Recognition in Infrared Road Images Using Improved Lightweight Model Based on MobileNetV2. *Journal of the Korea Institute of Information and Communication Engineering*, *25*(12), 1835-1845.

Sultani, W., & Shah, M. (2021). Human action recognition in drone videos using a few aerial training examples. *Computer Vision and Image Understanding*, *206*, 103186.

Park, G. Y., Lee, S. H., Kim, E. J., & Yun, B. Y. (2017). A case study on meteorological analysis of freezing rain and black ice formation on the load at winter. *Journal of Environmental Science International*, *26*(7), 827-836.

Park, K.W. & Cho, B.C. (2021). *Discovering and Preventing Black Ice using AI and Big Data*. n.p.: Korea Transport Institute.

Wang, X., He, N., Hong, C., Wang, Q., & Chen, M. (2023). Improved YOLOX-X based UAV aerial photography object detection algorithm. *Image and Vision Computing*, *135*, 104697.

Wang, Z., Cai, Z., & Wu, Y. (2023). An improved YOLOX approach for low-light and small object detection: PPE on tunnel construction sites. *Journal of Computational Design and Engineering*, *10*(3), 1158-1175.

Zhang, C., Nateghinia, E., Miranda-Moreno, L. F., & Sun, L. (2022). Winter road surface condition classification using convolutional neural network (CNN): visible light and thermal image fusion. *Canadian Journal of Civil Engineering*, *49*(4), 569-578.